Preparation of Sb doping ZnO: optical and structural evaluation on Variations Layer Thickness

Nurdin Siregar[1*], Alkafi Maas Siregar[2*] and Makmur Sirait[3*]

{ [1]siregarnurdin@unimed.ac.id, [2]alkhafi@unimed.ac.id, [3]maksir@unimed.ac.id}

Department of Physics, Faculty of Mathematics and Natural Sciences, Universitas Negeri Medan. Jl. Willem Iskandar Medan Estate, Medan 20221, Indonesia.

Abstract: By a sol-gel followed with spin coating technique, Sb doping thin films with varying coating thicknesses have been successfully synthesized. Crystal size determined by XRD analysis of Sb doping ZnO thin films with coating thickness variations ranging from 17.77 nm to 27.98 nm and a hexagonal wurtize-shaped crystal structure. The SEM analysis revealed that the thickness of the Sb doping ZnO thin films varied between 6.5 and 10.4 μm. The surface of Sb doping ZnO thin films reveals that the layer thickness increases as the crystallite grains appear round, nearly uniform, and dense, and there are almost no visible pores. UV-Vis analysis revealed that the transmittance value of all Sb doping ZnO thin films was greater than 80%. The energy band gap for all samples was 3.20 eV, and the thickness of Sb doping ZnO thin film had no effect on the energy band gap value.

Keywords: Sb doping ZnO Thin Film, Layer Thickness, Sol-Gel, and Spin Coating

1 Introduction

The semiconducting material zinc oxide, or ZnO, is one of the most important II–IV group semiconductors. Due to its favorable optical, electrical, and piezoelectric properties, ZnO becomes attractive to be used in several applications such as in the sensor and solar cell fields [1-5]. ZnO thin films have drawbacks, including poor electrical propertie with a low conductivity value of 6.24×10^{-7} $(\Omega cm)^{-1}$ [6]. To increase its electrical conduction, ZnO is widely doped using extrinsic dopants. Different types of metal doping group IIIA, such as boron, aluminum, gallium, and indium can be substituted to ZnO host structure [7]. Antimony (Sb) as the dopant was chosen as a doping agent because it can replace Zn side with an extra hole [8]. Thin film preparation techniques include pulse laser deposition, molecular beam epitaxy, spray pyrolysis, sputtering, and sol-gel [9-14]. Sol-gel spin coating method is utilized because the equipment is simple and inexpensive, no need of a high vacuum, temperature process is

ICoSTA 2022, November 01-02, Medan, Indonesia

DOI 10.4108/eai.1-11-2022.2326226

relatively low, the uniform composition, the coating thickness is controllable, and the excellent microstructural [15].

There are a few studies on Sb doping ZnO thin films have been carried out, including[16] with variations in doping concentration, the result shows that ZnO semiconductors is n-type without doping and becomes p-type after doping with 0.2% of Sb. According to another work [17], with variations of thickness of thin film, demonstrating that the energy band gap gets smaller as the thickness layer increases. According to [18], the variations of the ZnO thickness is an increase in the thickness of the ZnO thin film layer as the crystal size increases and the band gap energy decreases. According to [19], with variations in the thickness of the ZnO thin film layer, the result is an increase in the thickness of the ZnO thin film layer as the band gap energy increases.

2 Experimental section

The gel was synthesized using the sol-gel method by dissolving zinc and antimony precursors into isopropanol solution. After that, the solution was stirred on hot-plate magnetic stirrer at 60 °C. Then, 2 ml of diethanolamine (DEA) was dropped and kept heating at 60 °C for 2 hours. The solution is then allowed to cool down naturally to room temperature. Finally, the gel looks transparent. The first coating was done by dropping the gel onto the FTO and spin using a spin coating machine at 4000 rpm for 30 seconds, then drying in a oven at 80 °C and holding for 3-5 minutes. The second and third layers are applied in the same way. For samples with a thickness of 5 layers and samples with a thickness of 7 layers, it is done in the same way. The calcination was executed in electric furnace at 500 °C with a heating time of 2 hours to produce of a thin film of Sb doping ZnO.

3 Results and Discussions

3.1. Microstructural analysis

The thickness and the morphology of the Sb doping ZnO thin film layer was recorded using SEM, as exhibited in Figure 1 and Figure 2, respectively. The results of which show that the layer thickness increases as the spherical crystallite grains become visible. and is almost uniform and compact, consisting of grains that have a low interparticle boundary density and almost no visible porosity. The smaller grains get sufficient energy to move and form new bigger grains. As a result of diffusion between these grains, necking will form, which results in a reduction in the boundaries between grains and porosity so that the surface of the thin film looks smoother.

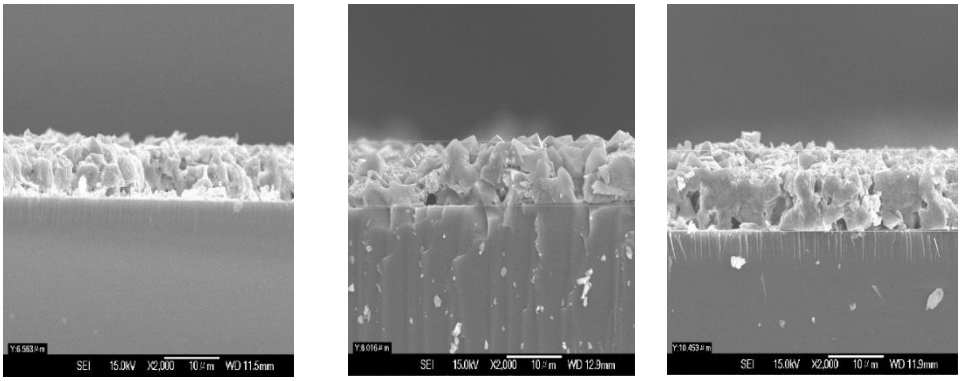

(a) **(b)** **(c)**

Figure 1. SEM photo of the thickness of the Sb doping ZnO sample: a) 3 layers. b) 5 layers, and c) 7 layers

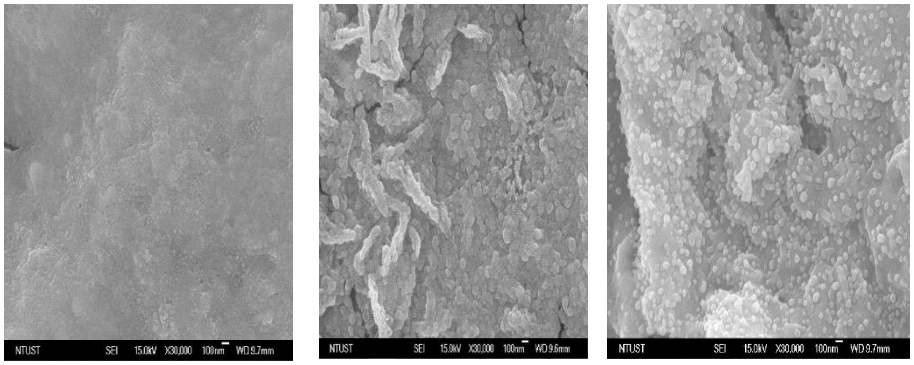

(a) **(b)** **(c)**

Figure 2. SEM images of Thin Film Sb doping ZnO surface Sb doping ZnO at various thickness layers a. 3 layers. b. 5 layers, and c. 7 layers

Based on Figure 1, the thickness of the sample is obtained, the results are listed in Table 1.

Table 1. Thickness of the Sb doping ZnO at various thickness layers

Sample	Layer Thickness (μm)
3 Layer	6.5
5 Layer	8.0
7 Layer	10.4

Based on Table 1, it is seen clesrly that the thickness of the layer increases with increasing the number of layers. This is due to the higher the number of layers, the more constituent atoms there will be, and so does the frequency of collisions of light particles with atoms, which occur more frequently, so that it is increasingly difficult for light to pass through the layers, and because the thickness of the layers formed increases, which causes less transparency. This is due to the increasing number of ZnO molecules involved, which affects the agglomeration process.

3.2. EDS analysis

The composition in the sample for various layer thicknesses, EDS analysis was conducted and the result is presented in Figure 3. The EDS spectrum of Sb doping ZnO at various layer thicknesses with Zn and O peaks is very clear throughout the EDS spectrum, while the Sb peak is weak due to the much lower concentration.

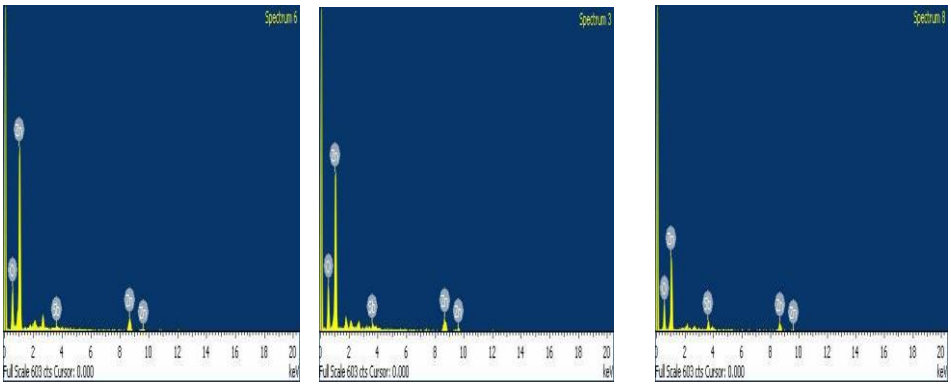

(a) **(b)** **(c)**

Figure 3. EDS spectra of Sb doping ZnO with thickness: a. 3 layers. b. 5 layers, and c. 7 layers

The atomic percentage of each element of each sample is tabulated in Table 2.

Table 2. Atomic percentage Zn, Sb and O in the Sb doping ZnO samples.

Sample	Sb (%)	Zn (%)	O (%)
6.5 μm	1.04	47.31	51.66
8.0 μm	3.38	37.45	59.16
10.4 μm	5.30	36.16	58.57

EDS measurements for samples with varying thicknesses of Sb doping ZnO thin films (6.5; 8.0 and 10.4 μm) indicated that the percentage of Zn contained in the ZnO thin films was the highest at 47.31% at a layer thickness of 6.5 μm and as low as 36.16% at a layer thickness of 10.4 μm. The highest O percentage was 59.16% at 8.0 μm layer thickness and the lowest was 51.66% at 6.5 μm layer thickness. The EDS results indicated that the incorporation of the Sb in the ZnO host.

3.3. Crystal Structure analysis

Figure 4 demonstrates XRD pattern of Sb doping ZnO thin film samples with varying thicknesses. This analysis shows that all samples possess the same peaks with orientation of (100), (002), and (101) planes. It also shows the same preference growth peak of (101). These data confirm that all the Sb doping ZnO has a wurtzite crystal structure according to the ZnO standard data on JCPDS card No. 36-1451[20,21]. These results show that the thickness of the layer does not change the crystal structure.

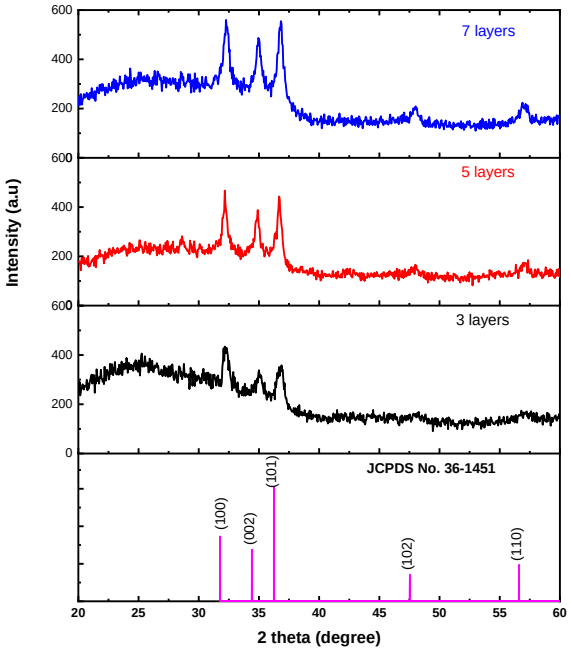

Figure 4. XRD pattern of Sb doping ZnO at various thickness layers

Table 3 shows the crystal properties of Sb doping ZnO, where crystallite size was obtained using the Debye Scherrer formula [22]

Table 3. Crystal properties of Sb doping ZnO at various thickness layers

Sample	Phase	Peak		Crystallite size (nm)
		$2\theta\ (degree)$	FWHM (rad)	
3 layers	ZnO	32.2	0.503	17.77
5 layers	ZnO	32.2	0.420	27.98
7 layers	ZnO	32.3	0.501	18.47

If the Full width half maximum (FWHM) value is low, the crystal size will be large, and vice versa. Based on Table 2, it is observed that the crystal size enhances with increasing number of layers to 5 layers, then begins to decrease when the number of layers is further going up to 7 layers. After the sample has undergone heating treatment, the collisions of light particles with atoms are more frequent, making it increasingly difficult for light to pass through. This is because the crystallite size get bigger. According to the results of previous works [23–25], the thickness of the layer affects the size of the crystal

3.4. Optical analysis

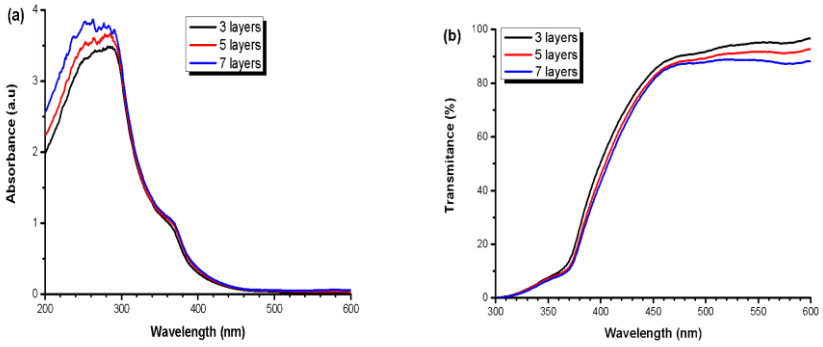

(a) **(b)**

Figure 5. a. Absorbance and b. Transmittance Spectra of Sb doping ZnO at various thickness layers

Figure 5a exhibits the absorption spectra of Sb-doping ZnO. It can be observed that the thickness of the sample increases as the absorption value of Sb doping ZnO thin films increases. This is because the less transparent the sample, the more ZnO:Sb molecules are involved in the visible light absorption process, so that the absorbance value at the same wavelength will be greater in thicker samples. All samples exhibited a sharp decrease in absorbance values between 280 and 420 nm, which corresponds to an ultraviolet wavelength area, and an increase in thickness of the layer caused the absorption edge to shift toward the region with shorter wavelengths. In Figure 5.b, the transmittance spectra of all samples demonstrates a sharp elevate in transmittance at wavelength range of 370 – 450 nm and a decrease in transmittance with increasing layer thickness. All Sb doping ZnO thin film samples have transmittance values greater than 80%, enabling their use in solar cells. According to [26], solar cells are capable of utilizing thin-film transmittance values of a high order. The relationship between absorption and energy photon of materials with a direct bandgap is as follows [27].

$$(\alpha hv)^2 = C_D(hv - E_{opt}) \quad (2)$$

On the basis of the Tauc Plot method, the bandgap energy of Sb doping ZnO with varying layer thicknesses is determined; the results are displayed in Figure 6.

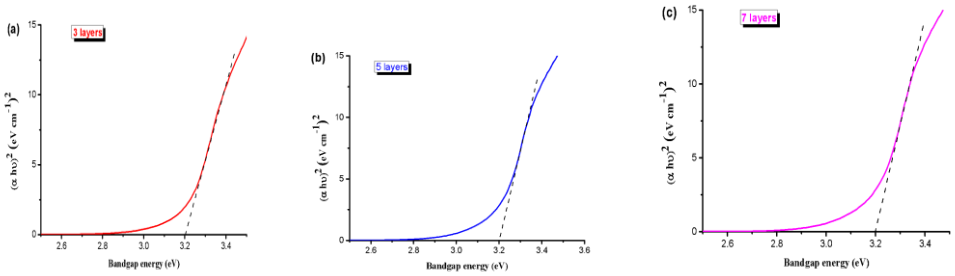

(a) (b) (c)

Figure 6. Bandgap determination based on Tauc Plot of Sb doping ZnO at various thickness layers a. 3 layers. b. 5 layers, and c. 7 layers

Table 4. Energy band gap of the Sample Sb doping ZnO at various thickness layers

Sample	Energy Band gap (eV)
6.5	3.20
8.0	3.20
10.4	3.20

Table 4 demonstrates the thickness of Sb doping ZnO thin film had no effect on the energy band gap value, as this value is only affected by the material employed. The bandgap energy degrades as the thickness of the thin film layer increases [17,18]. Variations of ZnO thickness result in increasing thickness as the energy band gap decreases. Moreover, according to [19], when the thickness of the ZnO thin film varies, the energy band gap increases as the ZnO thin film thickness increases.

4 Conclusion

By a sol-gel followed with spin coating technique, Sb doping ZnO thin films with varying coating thicknesses have been successfully synthesized. The thickness of the coating varies between 6.5 m, 8.0 m, and 10.4 m. Sb doping ZnO thin films have a hexagonal wurtzite crystal structure, with the largest crystal size measuring 27.98 nm at a layer thickness of 8.0. As the layer's thickness increases, it becomes more apparent that the crystallite grains are spherical, nearly uniform, compact, and composed of grains with a low interparticle boundary density and virtually no visible porosity. The transmittance value of Sb doping ZnO thin films is greater than 80% for all thicknesses. The energy band gap for all samples was 3.20 eV, and the thickness of Sb doping ZnO thin film had no effect on the energy band gap value.

Acknowledgments. Researchers would like to thank the leadership of Universitas Negeri Medan for their encouragement and financial support from the Public Service Agency (BLU) so that we can complete this research.

References

[1] Siregar, N., Panggabean, J.H., Sirait, M., Rajagukguk, J., Gultom, N.S. and Sabir, F.K.,. Fabrication of dye-sensitized solar cells (DSSC) using Mg-doped ZnO as photoanode and extract of rose myrtle (Rhodomyrtus tomentosa) as natural dye. International Journal of Photoenergy, 2021, 4033692

[2] Fierro, J.L.G. (2006) Metal Oxides: Chemistry & Applications. 6000 Broken Sound Parkway NW, Suite 300, Taylor & Francis Group

[3]. Saravanakumar, M., Agilan, S. and Muthukumarasamy, N. 2014. Effect of Annealing Temperature on Characterization of ZnO thin films by sol-gel method. International Journal of Chem Tech Research Coden (USA), 2014 6(5).

[4]. Siregar, N. and Sirait, M., Synthesis and optical properties of Sb doping ZnO thin film by sol-gel spin coating method. In Journal of Physics: Conference Series, 2022 (Vol. 2193, No. 1, p. 012063). IOP Publishing.

[5]. Suwanboon, S., Tanattha, R. and Tanakorn, R. Fabrication and properties of nanocrystalline zinc oxide thin film prepared by sol-gel method. J Sci Technol, 2008 30, pp.65-69.

[6]. Sugianto., Zannah, R., Mahmudah, S.N., Astuti, B., Putra, N.M.D., Wibowo, A.A., Marwoto, P., Ariyanto, D., Wibowo, E. 2016. Pengaruh Temperatur Aluminium Oksida. Jurnal MIPA 39 (2):115-122. http://journal. unnes. ac.id/nju/index.php/JM

[7]. Jana, S., Vuk, A.S., Mallick, A., Orel, B., Biswas, P.K. 2011. *Effect of Boron Doping on Optical Properties of Sol-Gel Based Nanostructured Zinc Oxide Films on Glass.* Materials Research Bulletin.(46) : 2392-2397.
[8]. Sinornate, W., Mimura, H dan Pecharapa, W. 2019. Role of Sb-dopant on Physical and Optical Properties of ZnO Thin Film Deposited by Sol-gel-based Coating Method. Chiang Mai J. Sci. 46(5)
[9] George, A. (2010). Microstructururе and field emission characteristics of ZnO nanoneedles grown by physical vapor deposition. Elsevier Materials Chemistry and Physics Vol 123.
[10]. Ali AK., Hussain., Kadhim A. Aadim, Hiba M. Slma. 2014. Structural and optical properties of ZnO doped Mg thin films deposited by pulse laser deposition (PLD). *Iraqi Journal of Physics, 2014 Vol.12, No.25, PP. 56-61*
[11]. Changzheng, Z. 2009. Effect of the oxygen pressure on the microstructure and optical properties of ZnO film prepared by laser molecular beam epitaxy. Elsevier Physics B 404
[12]. Kulandaisamy, AJ, JR Reddy, P. Srinivasan, KJ Babu, GK Mani, P. Shankar, and JBB Rayappan. 2016. "Room Temperature Ammonia Sensing Properties of ZnO Thin Films Grown by Spray Pyrolysis: Effect of Mg Doping." *Journal of Alloys and Compounds* 688:422–29.
[13]. Kumar, Y., Garcia, JE, and Singh, F. 2012. Influence of mesoporus substrate morphology on structural, optical and electrical properties of RF Sputtered ZnO layer deposited over porous silicon nanostructure. Applied Surface Science. Volume 258.
[14]. Sengupta, J., Ahmed, A., Labar, R. 2013. Structural and optical properties of post annealed Mg doped ZnO thin films deposited by the sol–gel method. Materials Letters109(2013)265–268. Elsevier.
[15]. Siregar, N., Motlan and Johnny Panggabean, J. 2019. The effect magnesium (Mg) on structural and optical properties of ZnO:Mg thin film by sol-gel spin coating method. The 4th International Conference on Applied Physics and Materials Application. Journal of Physics: Conference Series **1428** (2020) 012026. IOP Publishing. doi:10.1088/1742-6596/1428/1/012026
[16]. Caglar, Y., Caglar, M., Ilican, S. 2018. XRD, SEM, XPS studies of Sb doped ZnO films and electrical properties of its based Schottky diodes. Optics 164, 424–432. Elsevier.
[17]. Mia, MD. N. H., Rana, S.M., Pervez, MD. F., Rahman, M.R., Hosain, MD. K., Mortuza, A.AL., Basher, M.K., Hoq, M. 2017. Preparation and spectroscopic analysis of zinc oxide nanorod thin films of different thicknesses. Material Science-Poland.
[18]. Kumar, V., Singh, N., Mehra, R.M., Kapoor, A., Purohit, L.P., Swart, H.C. 2013. Role of film thickness on the properties of ZnO thin film grown by sol-gel methods. Thin Solid Films. 161-165. Elsevier.
[19]. Nithya, N dan Radhakkrisshnan. 2012. Effect of Thickness on the Properties ZnO Thin Films. Pelagia Research Library. Advances in Applied Science Research, 3 (6):4041=4047
[20]. Gultom, N.S., Abdullah, H. and Kuo, D.H., 2020. Phase transformation of bimetal zinc nickel oxide to oxysulfide photocatalyst with its exceptional performance to evolve hydrogen. Applied Catalysis B: Environmental, 272, p.118985.
[21]. Jianguo, Lv., Huang, K., Chen, X., Zhu, J., Wang, L., Song, X., Sun, Z. 2011. Effect of preheating temperatures on microstructure and optical properties of Na-doped ZnO thin films by sol-gel process. Superlattices and Microstructures 49.
[22]. Gultom, N.S., Silitonga, M.Z. and Kuo, D.H., 2022. Bimetallic Cobalt–Nickel Electrode Made by a Sputtering Technique for Electrocatalytic Hydrogen Evolution Reaction: Effect of Nickel Ratios. ACS Applied Energy Materials, 5(7), pp.8658-8668.
[23]. Saleem, M., Fang, L., Ruan, H.B., Wu1, F., Huang, Q.L., Xu, C.L dan Kong, C.Y. 2012. Effect of zinc acetate concentration on the structural and optical properties of ZnO thin films deposited by Sol-Gel method International Journal of Physical Sciences Vol. 7(23), pp. 2971-2979.
[24]. Gayen, R.N., Sarkar, N., Hussain, S., R, Bhar and A.K. Pal. 2011. ZnO Films Prepared By Modified Sol-Gel Technique. Vo; 49. Pp. 470-477.
[25]. Amutha, C., Dhanalaksmi, A., Lawrence, B., Kulathuraan, K., Ramadas, V., Natarajan, B. 2014. Influence of Concentration on Structural and Optical Characteristics of Nanocrystalline ZnO Thin Films Snthesized b Sol-Gel Dip Coating Method. Progress in Nanotechnology and Nanomaterials, Vol 3

[26] Bekele, E.T., Zereffa, E.A., Gultom, N.S., Kuo, D.H., Gonfa, B.A. and Sabir, F.K., 2021. Biotemplated synthesis of titanium oxide nanoparticles in the presence of root extract of Kniphofia schemperi and its application for dye sensitized solar cells. International Journal of Photoenergy, 2021.
[27]. Gultom, N.S., Abdullah, H., Xie, J.C., Shuwanto, H. and Kuo, D.H., 2022. Improved Hydrogen Production Rate of a Nickel-Doped Zinc Indium Oxysulfide Visible-Light Catalyst: Comparative Study of Stoichiometric and Nonstoichiometric Compounds. ACS Applied Energy Materials, 5(2), pp.1755-1766.